



Year: 2016

Incorporation of staphylococci into titanium-grown biofilms: an in vitro "submucosal" biofilm model for peri-implantitis

Thurnheer, Thomas ; Belibasakis, Georgios N

Abstract: OBJECTIVES Staphylococcus spp. are postulated to play a role in peri-implantitis. This study aimed to develop a "submucosal" in vitro biofilm model, by integrating two staphylococci into its composition. MATERIALS AND METHODS The standard "subgingival" biofilm contained *Actinomyces oris*, *Fusobacterium nucleatum*, *Streptococcus oralis*, *Veillonella dispar*, *Campylobacter rectus*, *Prevotella intermedia*, *Streptococcus anginosus*, *Porphyromonas gingivalis*, *Tannerella forsythia* and *Treponema denticola*, and was further supplemented with *Staphylococcus aureus* and/or *Staphylococcus epidermidis*. Biofilms were grown anaerobically on hydroxyapatite or titanium discs and harvested after 64 h for real-time polymerase chain reaction, to determine their composition. Confocal laser scanning microscopy and fluorescence in situ hybridization were used for identifying the two staphylococci within the biofilm. RESULTS Both staphylococci established within the biofilms when added separately. However, when added together, only *S. aureus* grew in high numbers, whereas *S. epidermidis* was reduced almost to the detection limit. Compared to the standard subgingival biofilm, addition of the two staphylococci had no impact on the qualitative or quantitative composition of the biofilm. When grown individually in the biofilm, *S. epidermidis* and *S. aureus* formed small distinctive clusters and it was confirmed that *S. epidermidis* was not able to grow in presence of *S. aureus*. CONCLUSIONS *Staphylococcus aureus* and *S. epidermidis* can be individually integrated into an oral biofilm grown on titanium, hence establishing a "submucosal" biofilm model for peri-implantitis. This model also revealed that *S. aureus* outcompetes *S. epidermidis* when grown together in the biofilm, which may explain the more frequent association of the former with peri-implantitis.

DOI: <https://doi.org/10.1111/clr.12715>

Posted at the Zurich Open Repository and Archive, University of Zurich

ZORA URL: <https://doi.org/10.5167/uzh-113607>

Journal Article

Published Version



The following work is licensed under a Creative Commons: Attribution-NonCommercial 4.0 International (CC BY-NC 4.0) License.

Originally published at:

Thurnheer, Thomas; Belibasakis, Georgios N (2016). Incorporation of staphylococci into titanium-grown biofilms: an in vitro "submucosal" biofilm model for peri-implantitis. *Clinical Oral Implants Research*, 27(7):890-895.

DOI: <https://doi.org/10.1111/clr.12715>

Thomas Thurnheer
Georgios N. Belibasakis

Incorporation of staphylococci into titanium-grown biofilms: an *in vitro* "submucosal" biofilm model for peri-implantitis

Authors' affiliations:

Thomas Thurnheer, Georgios N. Belibasakis,
Section of Oral Microbiology and Immunology,
Institute of Oral Biology, Center of Dental
Medicine, University of Zürich, Zürich,
Switzerland

Corresponding author:

Prof. Georgios N. Belibasakis
Section of Oral Microbiology and Immunology,
Institute of Oral Biology, Center of Dental
Medicine, University of Zürich, Plattenstrasse 11,
CH-8032 Zürich, Switzerland
Tel.: +41 44 634 33 06
Fax: +41 44 634 30 90
e-mail: george.belibasakis@zzm.uzh.ch

Key words: biofilms, *in vitro* model, peri-implantitis, titanium surface

Abstract

Objectives: *Staphylococcus* spp. are postulated to play a role in peri-implantitis. This study aimed to develop a "submucosal" *in vitro* biofilm model, by integrating two staphylococci into its composition.

Materials and methods: The standard "subgingival" biofilm contained *Actinomyces oris*, *Fusobacterium nucleatum*, *Streptococcus oralis*, *Veillonella dispar*, *Campylobacter rectus*, *Prevotella intermedia*, *Streptococcus anginosus*, *Porphyromonas gingivalis*, *Tannerella forsythia* and *Treponema denticola*, and was further supplemented with *Staphyococcus aureus* and/or *Staphylococcus epidermidis*. Biofilms were grown anaerobically on hydroxyapatite or titanium discs and harvested after 64 h for real-time polymerase chain reaction, to determine their composition. Confocal laser scanning microscopy and fluorescence *in situ* hybridization were used for identifying the two staphylococci within the biofilm.

Results: Both staphylococci established within the biofilms when added separately. However, when added together, only *S. aureus* grew in high numbers, whereas *S. epidermidis* was reduced almost to the detection limit. Compared to the standard subgingival biofilm, addition of the two staphylococci had no impact on the qualitative or quantitative composition of the biofilm. When grown individually in the biofilm, *S. epidermidis* and *S. aureus* formed small distinctive clusters and it was confirmed that *S. epidermidis* was not able to grow in presence of *S. aureus*.

Conclusions: *Staphyococcus aureus* and *S. epidermidis* can be individually integrated into an oral biofilm grown on titanium, hence establishing a "submucosal" biofilm model for peri-implantitis. This model also revealed that *S. aureus* outcompetes *S. epidermidis* when grown together in the biofilm, which may explain the more frequent association of the former with peri-implantitis.

Peri-implant diseases are infectious diseases that affect the tissues surrounding the dental implants (Mombelli & Lang 1998). Peri-implant mucositis and peri-implantitis are analogous to gingivitis and periodontitis of natural teeth, exhibiting several similarities but also differences (Belibasakis 2014). While the pathological events that govern peri-implantitis qualitatively resemble periodontitis, the extent and rapidity of the tissue destruction is more pronounced in peri-implantitis (Heitz-Mayfield & Lang 2010; Belibasakis et al. 2015). In addition, the microbial composition of peri-implantitis biofilms resembles that of periodontitis (Mombelli & Decaillet 2011). However, with the increasing use of molecular technologies based on metagenomics, it is likely that more differences will be identified, and a broader

diversity will be revealed (Charalampakis & Belibasakis 2015; Faveri et al. 2015).

Several studies admittedly show that some taxa identified in peri-implantitis are less common in periodontitis, including *Staphylococcus aureus* and *Staphylococcus epidermidis* (Rams & Link 1983; Rams et al. 1991; Renvert et al. 2007; Charalampakis et al. 2012; Persson & Renvert 2014; Zhuang et al. 2014). The biological rationale behind the involvement of *Staphylococcus* spp. in peri-implantitis is their capacity to efficiently attach onto titanium surfaces (Harris & Richards 2004), and contribute to the medical device infections, which are biofilm-associated (Costerton et al. 2005). In this light, *S. aureus* is a potential pathogen of relevance to orthopaedics, as it exhibits a strong association to osteomyelitis and orthopaedic

Date:

Accepted 18 September 2015

To cite this article:

Thurnheer T, Belibasakis GN. Incorporation of staphylococci into titanium-grown biofilms: an *in vitro* "submucosal" biofilm model for peri-implantitis.
Clin. Oral Impl. Res. 27, 2016, 890–895
doi: 10.1111/clr.12715

implant infection (Arciola 2009). Regarding titanium-based dental implants, *S. aureus* can be detected on their surface within an hour following surgical insertion (Salvi et al. 2008). With regard to peri-implant infections, it is indeed confirmed that *S. aureus* or *Staphylococcus anaerobius* are found at higher numbers in biofilm obtained from implants with peri-implantitis, than peri-implant health (Persson & Renvert 2014).

Multi-species *in vitro* biofilm models can serve as useful tools in the study of various polymicrobial infections. A “subgingival” biofilm model consisting of 10–11 periodontitis-associated species grown on hydroxyapatite (HA) discs was developed to address questions related to the aetiology of periodontitis (Guggenheim et al. 2009; Ammann et al. 2012). Such questions are pertinent to the interaction between species in the biofilm (Ammann et al. 2013a,b; Bao et al. 2014, 2015) or the interaction of the biofilm itself with host cells or tissues (Belibasakis & Guggenheim 2011; Belibasakis et al. 2011a,b, 2013a,b; Bostanci et al. 2011; Thurnheer et al. 2014; Willi et al. 2014). As peri-implantitis is a newly emerged oral infection (Heitz-Mayfield & Lang 2010; Belibasakis 2014), there is a need for the establishment of a biofilm model of relevance to this disease. Therefore, the aim of this study was to convert our standard periodontitis “subgingival” biofilm model into a peri-implantitis “submucosal” one, by incorporating *S. aureus* and/or *S. epidermidis* into its composition, and replacing the biofilm growth surface of hydroxyapatite with titanium. This new model would serve as an important tool for various applications related to the study of peri-implantitis.

Materials and methods

Formation of *in vitro* biofilms

For this study, our standard 10-species “subgingival” biofilm model was used abiding a slightly modified protocol as described previously (Guggenheim et al. 2009; Ammann et al. 2012; Thurnheer et al. 2014). In brief, biofilms were grown in medium, consisting of 60% of processed whole unstimulated pooled saliva, 30% modified fluid universal medium (mFUM) (Gmur & Guggenheim 1983) and 10% heat inactivated human serum. Incubation was carried out for 64 h under anaerobic conditions at 37 °C. The standard subgingival *in vitro* biofilm was composed of *Actinomyces oris* (OMZ 745; formerly *Actinomyces naeslundii*), *Campy-*

lobacter rectus OMZ 698, *Fusobacterium nucleatum* subsp. *nucleatum* OMZ 598, *Porphyromonas gingivalis* ATCC 33277^T (OMZ 925), *Prevotella intermedia* ATCC 25611^T (OMZ 278), *Streptococcus anginosus* ATCC 9895 (OMZ 871), *Streptococcus oralis* SK248 (OMZ 607), *Tannerella forsythia* OMZ 1047, *Treponema denticola* ATCC 35405^T (OMZ 661) and *Veillonella dispar* ATCC 17748^T (OMZ 493). This standard biofilm was supplemented with either *S. epidermidis* ATCC 14990 (OMZ 423) (treatment 1), or *S. aureus* ATCC 25923 (OMZ 1122) (treatment 2) or a mixture of the two staphylococci (treatment 3) or a mixture of the latter and an additional boost inoculation of *S. epidermidis* after 16 h (treatment 4). All strains were maintained on Columbia Blood Agar (CBA) plates, with the exception of *T. forsythia* and *T. denticola* that were maintained in liquid growth media as described previously (Ammann et al. 2012). Biofilms were grown in 24-well polystyrene cell culture plates on hydroxyapatite (Ø 9 mm; Clarkson Chromatography Products, South Williamsport, PA, USA) and titanium discs (TiUnite, Nobel Biocare, Kloten Switzerland) that had been preconditioned (pellicle-coated) in 1 ml of pasteurized whole unstimulated saliva, pooled from individual donors, and incubated for 4 h at room temperature. The same saliva batch was used in all experimentations. To initiate biofilm formation, the pellicle-coated discs were covered with 1 ml of growth medium (see above), and 200 µl of a microbial suspension prepared from equal volumes and densities of each strain, corresponding to OD₅₅₀ = 1.0. The carbohydrate concentration in FUM was

0.3% (w/v) glucose. After 16 h of incubation, the growth medium was renewed, along with adding 50 µl of *T. denticola* liquid culture as well as 50 µl of *S. epidermidis* culture (OD₅₅₀ = 1.0) in treatment 4 (see above). At 16, 20, 24, 40, 44 and 48 h, biofilms were washed by three consecutive dips in 2 ml of sterile physiological saline. Fresh medium was provided after 16 and 40 h. After 64 h, the biofilms were dip-washed again prior to harvesting for quantification by real-time quantitative PCR (qPCR) or processing for fluorescence in situ hybridization (FISH) staining and confocal laser scanning microscopy (CLSM) analyses, as described below.

Quantitative determination of the biofilm species

After 64 h of biofilm growth, the discs were vortexed vigorously for 1 min in 1 ml of 0.9% NaCl and then sonicated at 25W in a Sonifier B-12 (Branson Ultrasonic, Urdorf, Switzerland) for 5 s, to harvest the adherent biofilms. The resulting bacterial suspensions were then used for quantification by qPCR as described earlier (Ammann et al. 2013a,b). Primer sequences and properties of the standard 10-species biofilm are given in Table 1. The staphylococci were quantified using the microbial DNA qPCR assays for *S. epidermidis* and *S. aureus* (Qiagen Instruments, Hombrechtikon, Switzerland; Cat. no. BPID00316A and BPID00314A, respectively).

Staining of biofilms

Biofilms were stained by FISH using Cy3- or FAM-labelled probes following the protocols described before (Thurnheer et al. 2004; Thurnheer & Belibasakis 2015). Probe

Table 1. Primer sequences and properties

Organism	Sequence (5' → 3')	Strand on template	T _m (°C)	Product length (bases)
<i>Actinomyces oris</i>	GCCTGTCCCTTTGTGGGTGGG	+	59.57	71
	GCGGCTGCTGGCAGTAGTT	–	60.32	
<i>Campylobacter rectus</i>	TCACCGCCCGTCACACCATG	+	59.35	57
	CCGGTTTGGTATTTGGGCTTCGAGT	–	59.5	
<i>Fusobacterium nucleatum</i>	CGCCCGTCACACCACGAGA	+	59.04	75
	ACACCCTCGGAACATCCCTCTTAC	–	59.48	
<i>Porphyromonas gingivalis</i>	GCGAGAGCCTGAACCAGCCA	+	59.07	90
	ACTCGTATCGCCGTTATCCCGTA	–	59.44	
<i>Prevotella intermedia</i>	GCGTGACAGATTACGGCCCTAT	+	59.61	68
	GGCACACGTGCCCCGTTTACT	–	60.24	
<i>Streptococcus anginosus</i>	ACCAGGTCTTGACATCCCGATGCTA	+	59.25	76
	CCATGCACACCTGTACCGGA	–	59.04	
<i>Streptococcus oralis</i>	ACCAGGTCTTGACATCCCTCTGACC	+	59.42	70
	ACCACCTGTACCTCTGTCCCG	–	59.85	
<i>Treponema denticola</i>	TAAAGGACAGCTTGCTCACCCCTA	+	58.84	55
	CACCCACGCGTTACTCACCAGTC	–	59.76	
<i>Tannerella forsythia</i>	CGATGATACGCGAGGAACCTTACCC	+	59.07	72
	CCCAGGGAAGAAAGCTCTCACTCT	–	58.01	
<i>Veillonella dispar</i>	CCGGGCTTGTACACACCG	+	59.7	62
	CCCACCGCTTTGGGCACTT	–	59.83	
T _m melting temperature.				

sequences and formamide concentrations used for the hybridizations, as well as the NaCl concentrations of the washing buffers, are given in Table 2. For counterstaining, biofilms were stained using 3 µM Syto 59 (Invitrogen, Lucerne, Switzerland) (20 min, room temperature, in the dark), following the FISH procedure. After staining, the samples were embedded upside-down on chamber slides in 100 µl of Mowiol 4-88 (Calbiochem-Novabiochem, San Diego, CA, USA) (Guggenheim et al. 2001).

Confocal laser scanning microscopy (CLSM)

Stained biofilms were examined by CLSM at randomly selected positions using a Leica TCS SP5 microscope (Leica Microsystems, Wetzlar, Germany) fitted with an Ar laser (458 nm/476 nm/488 nm/496 nm/514 nm excitation), and a He-Ne laser (561 nm/594 nm/633 nm excitation). Filters were set to 500–540 nm to detect FAM, to 570–630 nm for Cy3 and to 660–710 nm for Syto 59. Confocal images were obtained using ×63 (numeric aperture 1.30) glycerol immersion objective. Z-series were generated by vertical optical sectioning with the slice thickness set at 1.02 µm. Image acquisition was performed in ×8 line average mode. Scans were recombined and processed using Imaris 7.6.5 software (Bitplane, Zürich, Switzerland), without any qualitative changes to the raw images.

Statistical analyses

Three independent experiments were performed, and within each experiment every group was represented in triplicate biofilm cultures. Hence, statistics were performed on nine individual data points, deriving from the nine individual biofilm cultures per experimental group. The statistical significance of the differences in microbial numbers between the control group (standard 10-species “subgingival” biofilm) and the four treatments was evaluated by two-way analysis of variance (ANOVA), corrected by Tukey’s multiple comparisons test (significance level $P < 0.05$). Undetectable values were ascribed the lowest detection limit value of the assay to allow for logarithmic transformation.

Comparisons were performed between the control group and each experimental group, for each individual species. The data were analysed using the Prism version 6, statistical analysis software (GraphPad, La Jolla, CA, USA).

Results

A standard 10-species “subgingival” biofilm was used as the ground model for this study, grown either on HA or titanium discs. Firstly, biofilm growth on HA was investigated (Fig. 1a). When *S. aureus* or *S. epidermidis* was included in the initial inoculum, either individually or together, all of the remaining original 10 species were grown unimpeded in the biofilm. Significant ($P < 0.05$) changes in *C. rectus*, *P. gingivalis* and *T. forsythia* numbers were observed only when *S. epidermidis* was re-inoculated (i.e. “booster”) after 16 h following the initiation of biofilm formation. The numbers of *P. gingivalis* and *T. forsythia* were increased by 2.9-fold and 3.2-fold, respectively, when the two staphylococci were present in the biofilm, whereas *C. rectus* decreased by 6.1-fold. Yet, these changes in numbers remained within one step of the log₁₀ scale. Importantly, *S. aureus* was successfully incorporated and grown in the biofilm under any of the tested conditions. This was also the case for *S. epidermidis* when inoculated together with the 10 “subgingival” species. However, when *S. epidermidis* and *S. aureus* were inoculated together along with the 10 other species, the growth of the former was significantly inhibited by approximately 3 steps of the log₁₀ scale (Fig. 1a).

Biofilm formation on titanium surfaces was thereafter investigated in a similar manner (Fig. 1b). It was found that presence of *S. aureus* or *S. epidermidis* in the inoculum (together or individually) did not cause any changes in the numbers of the 10 original species after 64 h of biofilm growth. Accordingly, *S. aureus* and *S. epidermidis* were able to successfully grow as part of the biofilm, along with the other species. However, when

these two staphylococci were inoculated together, only *S. aureus* was able to grow in the biofilm, whereas the growth of *S. epidermidis* was suppressed.

This newly established biofilm model whereby *S. epidermidis* or *S. aureus* was able to integrate among the 10 “subgingival” species, was also analysed structurally by CLSM (Fig. 2). Technically, it was not possible to perform CLSM on the biofilm grown on titanium discs, as the biofilm displayed increased detachment from this surface during the execution of the FISH-staining protocol. Therefore, this analysis was performed only on the biofilms formed on HA discs. The structure and bacterial distribution of the 10-species (control) biofilm is visualized in Fig. 2a, whereas the presence of *S. epidermidis* (Fig. 2b) or *S. aureus* (Fig. 2c) was individually confirmed by FISH staining, using fluorescence-labelled 16S rRNA oligonucleotide probes (Table 2). In both staphylococci groups, there were small but distinctive bacterial cell clusters of the associated species (red colour), which were scattered across the biofilm mass (green colour). In the case where *S. aureus* and *S. epidermidis* were simultaneously co-inoculated (Fig. 2d), or when *S. epidermidis* was re-inoculated after 16 h (Fig. 2e), only *S. aureus* was identified in the biofilm, whereas *S. epidermidis* was not detectable. The distribution and clustering of *S. aureus* when co-inoculated with *S. epidermidis* did not differ from the biofilm group where *S. aureus* was inoculated alone. These findings corroborate the low detection levels of *S. epidermidis* by qPCR in the corresponding biofilm groups (Fig. 1).

Discussion

The present study established and characterized an *in vitro* multi-species “submucosal” biofilm model, which is of relevance to peri-implantitis. It is based on the advancement of the original 10-species “subgingival” biofilm grown anaerobically on HA discs (Guggenheim et al. 2009; Ammann et al. 2012, 2013a,b; Belibasakis & Thurnheer 2014). The novelty lies in the growth of the biofilm on titanium discs, as well as the incorporation of *S. aureus* or *S. epidermidis* individually in its structure. Staphylococci have allegedly been more associated with peri-implantitis than peri-implant health, or periodontitis (Heitz-Mayfield & Lang 2010; Belibasakis 2014). Studies have also shown that *S. aureus* DNA counts are greater on dental implants than on natural teeth, as

Table 2. Sequence and formamide concentrations for FISH Probes

Organism	Name	Label	FA* (%)	NaCl† (mM)	Sequence (5' → 3')	Source
<i>Staphyococcus aureus</i>	Saur229	Cy3	30	112	CTAATGCAGCGCGGATCC	‡
<i>Staphylococcus epidermidis</i>	Sepi229	FAM	30	112	CTAATGCGGCGCGGATCC	This study

*Formamide concentration in the hybridization buffer.

†Concentration of NaCl used in the washing buffer.

‡Thurnheer & Belibasakis (2015), Virulence 6, 258–64.

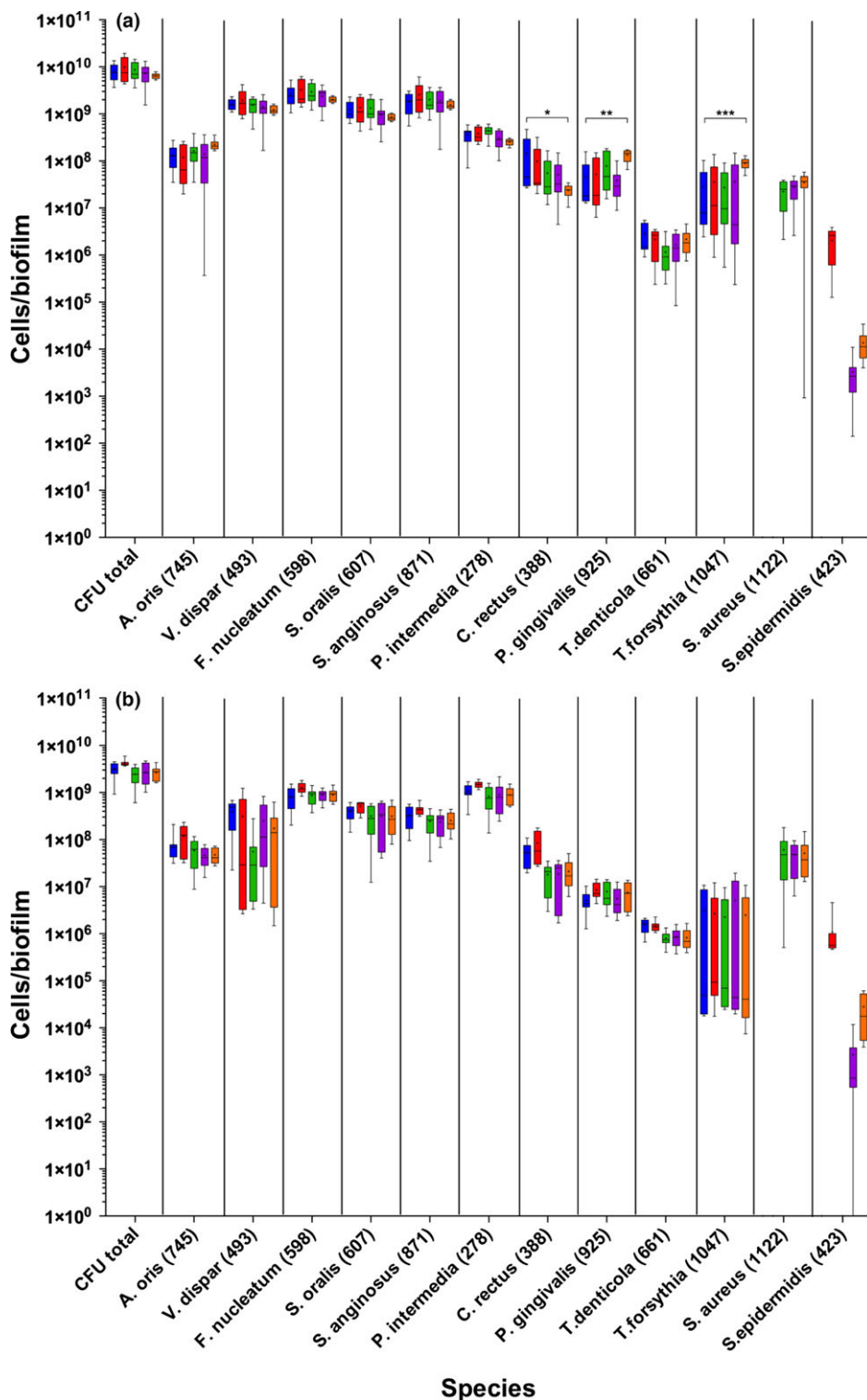


Fig. 1. Cells/biofilm of the standard 10-species subgingival biofilm grown on hydroxyapatite (a) or titanium discs (b) (control group; blue), containing additionally *Staphylococcus epidermidis* (treatment 1; red), or *Staphylococcus aureus* (treatment 2; green), or *S. epidermidis* + *S. aureus* (treatment 3; purple) or *S. epidermidis* + *S. aureus* + a boost inoculation of *S. epidermidis* after 16 h of growth (treatment 4; orange). Box plots represent cells/biofilm determined by qPCR. The OMZ strain number is provided in the parenthesis after the species names. Statistically significant differences compared with the control group are indicated with asterisks (* $P < 0.05$, ** $P < 0.01$, *** $P < 0.001$).

evaluated by DNA–DNA hybridization assays (Renvert et al. 2008). However, such methods should be considered with more caution due to potential cross-reactivity

between taxa that could lead to over-interpretation of the findings (Charalampakis & Belibasakis 2015). Yet, culture-dependent methods have confirmed the presence of

staphylococci in peri-implantitis, albeit rather infrequently (Leonhardt et al. 1999; Charalampakis et al. 2012). Hence, there is sufficient reasoning to incorporate further staphylococci into our 10-species experimental biofilm model. Formation of mono-species biofilms of *S. epidermidis* has previously been investigated in relation to titanium surfaces (Burgers et al. 2012).

Both *S. aureus* and *S. epidermidis* were able to grow as part of the biofilm, at numbers comparable to the other constituent “subgingival” species. Moreover, it was possible for the biofilms to grow on both HA and titanium surfaces, denoting that there is no selective advantage of the growth of this biofilm on one surface over the other. These results are in line with the recent observation that *S. aureus* can efficiently grow within a biofilm consisting of another six “supragingival” species, without affecting their numeric composition (Thurnheer & Belibasakis 2015). Within that biofilm, *S. aureus* appeared to localize in small and rather secluded clusters of its own species. This observation is very similar to the localization pattern of either *S. aureus* or *S. epidermidis* observed in the present “submucosal” biofilm. This may denote that staphylococci can grow in a sparse, yet distinctive, pattern as part of oral biofilms, without outcompeting in growth and spatial arrangement with the remaining constituent species, as has been shown in the case of *Escherichia coli* (Thurnheer & Belibasakis 2015).

A competition trend between the newly introduced staphylococci was also observed in the present study. That is, when *S. epidermidis* was co-inoculated with *S. aureus*, the former failed to grow in the biofilm. This trait was observed on both HA and titanium surfaces. Clearly, this denotes an ecological advantage of *S. aureus* over *S. epidermidis* under the present micro-environmental conditions. This may explain the more frequent detection of *S. aureus* than *S. epidermidis* in biofilms from sites with peri-implantitis (Mombelli & Decaillet 2011). Otherwise, there is also contrary evidence that the mono-species competition between *S. aureus* and *S. epidermidis* by means of quorum-sensing may generally be in favour of *S. epidermidis*, which might explain its predominance on skin and infections on indwelling medical devices (Otto et al. 2001). Yet, one has to consider that every micro-environmental niche of the human body is ecologically different and may therefore provide selective conditions for the growth of different bacteria, or their interactions with each other.

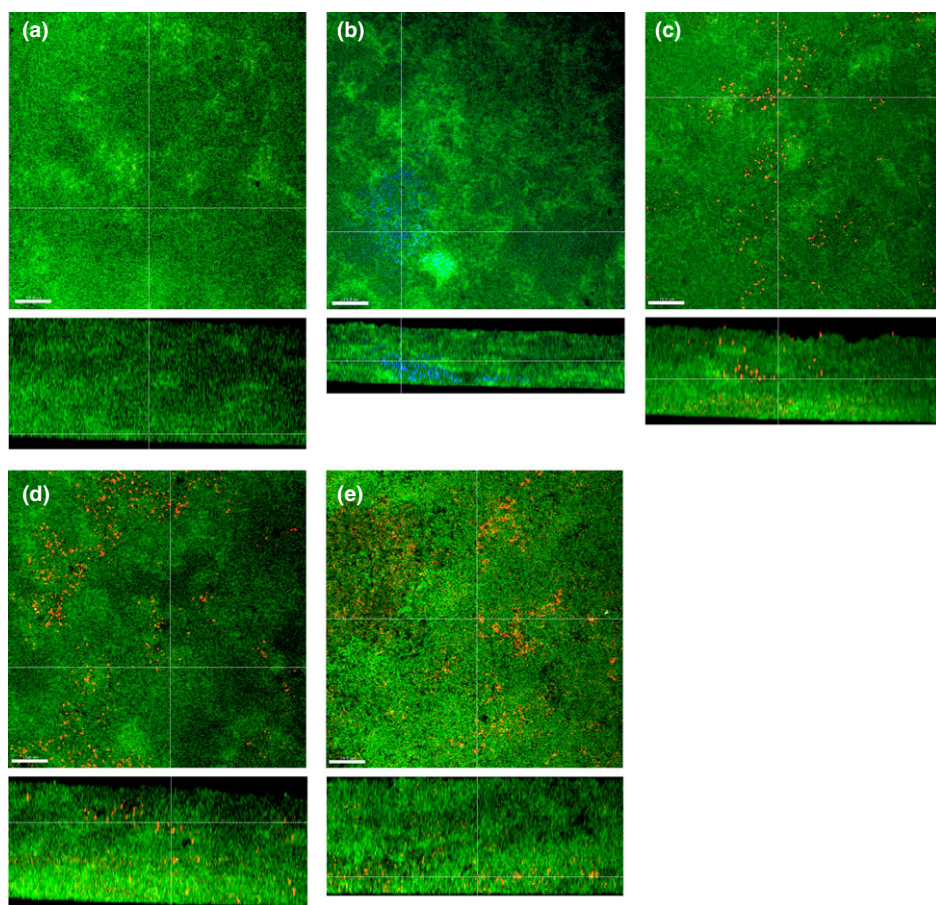


Fig. 2. CLSM images of the standard 10-species subgingival biofilm after 64 h of growth on hydroxyapatite discs (control group; a) containing additionally *Staphylococcus epidermidis* (treatment 1; b), or *Staphylococcus aureus* (treatment 2; c), or *S. epidermidis* + *S. aureus* (treatment 3; d) or *S. epidermidis* + *S. aureus* + a boost inoculation of *S. epidermidis* after 16 h of growth (treatment 4; e). Bacteria appear green due to DNA-staining using Syto 59. Due to FISH staining with 16S rRNA probes, Sepi229 and Saur229 *S. epidermidis* and *S. aureus* appear blue and red, respectively. The biofilm base in the cross sections is directed towards the top view. Scale = 15 µm.

Hence, within a “submucosal” oral biofilm, such as the one developed in this study, the

behavioural interaction between *S. aureus* and *S. epidermidis* can be different than on

skin. It is worth noting at this stage that, with the present experimental approach, it is not possible to gauge whether this effect was due to direct suppression of *S. epidermidis* by *S. aureus*, or a community effect of *S. aureus* on this polymicrobial species biofilm.

In conclusion, the present study has established and characterized “submucosal” biofilm model for peri-implantitis grown on titanium surfaces, by individually integrating *S. aureus* or *S. epidermidis*. The model can be used for testing potential modalities for the prevention or treatment of peri-implantitis, before being applied into the clinics. Moreover, this model also revealed a competitive interaction between *S. aureus* and *S. epidermidis* in oral biofilms, whereby the former outcompetes the growth of the latter. This is an interesting micro-ecological observation that may explain the more frequent detection of *S. aureus* than *S. epidermidis*, in peri-implantitis biofilms.

Acknowledgements: We would like to thank Mrs. Ruth Graf, Mr. André Meier and Mrs. Elpidia Plattner for their excellent technical assistance with the experimentations. We thank the Center of Microscopy and Image Analysis (ZMB) of the University of Zürich for their support with confocal microscopy, and Nobel Biocare Services AG (Switzerland) for providing the titanium discs used in this study. This study was supported by the authors’ Institute. The authors declare no conflict of interest.

References

- Ammann, T.W., Belibasakis, G.N. & Thurnheer, T. (2013a) Impact of early colonizers on in vitro subgingival biofilm formation. *PLoS ONE* **8**: e83090.
- Ammann, T.W., Bostanci, N., Belibasakis, G.N. & Thurnheer, T. (2013b) Validation of a quantitative real-time PCR assay and comparison with fluorescence microscopy and selective agar plate counting for species-specific quantification of an in vitro subgingival biofilm model. *Journal of Periodontal Research* **48**: 517–526.
- Ammann, T.W., Gmur, R. & Thurnheer, T. (2012) Advancement of the 10-species subgingival zurich biofilm model by examining different nutritional conditions and defining the structure of the in vitro biofilms. *BMC Microbiology* **12**: 227.
- Arciola, C.R. (2009) New concepts and new weapons in implant infections. *International Journal of Artificial Organs* **32**: 533–536.
- Bao, K., Belibasakis, G.N., Thurnheer, T., Aduse-Opoku, J., Curtis, M.A. & Bostanci, N. (2014) Role of *Porphyromonas gingivalis* gingipains in multi-species biofilm formation. *BMC Microbiology* **14**: 258.
- Bao, K., Bostanci, N., Selevsek, N., Thurnheer, T. & Belibasakis, G.N. (2015) Quantitative proteomics reveal distinct protein regulations caused by *Aggregatibacter actinomycetemcomitans* within subgingival biofilms. *PLoS ONE* **10**: e0119222.
- Belibasakis, G.N. (2014) Microbiological and immuno-pathological aspects of peri-implant diseases. *Archives of Oral Biology* **59**: 66–72.
- Belibasakis, G.N., Charalampakis, G., Bostanci, N. & Stadlinger, B. (2015) Peri-implant infections of oral biofilm etiology. *Advances in Experimental Medicine and Biology* **830**: 69–84.
- Belibasakis, G.N. & Guggenheim, B. (2011) Induction of prostaglandin E(2) and interleukin-6 in gingival fibroblasts by oral biofilms. *FEMS Immunology and Medical Microbiology* **63**: 381–386.
- Belibasakis, G.N., Guggenheim, B. & Bostanci, N. (2013a) Down-regulation of nlrp3 inflammasome in gingival fibroblasts by subgingival biofilms: involvement of *Porphyromonas gingivalis*. *Innate Immunity* **19**: 3–9.
- Belibasakis, G.N., Meier, A., Guggenheim, B. & Bostanci, N. (2011a) Oral biofilm challenge regulates the rankl-opg system in periodontal ligament and dental pulp cells. *Microbial Pathogenesis* **50**: 6–11.
- Belibasakis, G.N., Meier, A., Guggenheim, B. & Bostanci, N. (2011b) The rankl-opg system is differentially regulated by supragingival and subgingival biofilm supernatants. *Cytokine* **55**: 98–103.
- Belibasakis, G.N. & Thurnheer, T. (2014) Validation of antibiotic efficacy on in vitro subgingival biofilms. *Journal of Periodontology* **85**: 343–348.
- Belibasakis, G.N., Thurnheer, T. & Bostanci, N. (2013b) Interleukin-8 responses of multi-layer gingival epithelia to subgingival biofilms: role of the “red complex” species. *PLoS ONE* **8**: e81581.

- Bostanci, N., Meier, A., Guggenheim, B. & Belibasakis, G.N. (2011) Regulation of nlrp3 and aim2 inflammasome gene expression levels in gingival fibroblasts by oral biofilms. *Cellular Immunology* **270**: 88–93.
- Burgers, R., Wittecy, C., Hahnel, S. & Gosau, M. (2012) The effect of various topical peri-implantitis antiseptics on *Staphylococcus epidermidis*, *Candida albicans*, and *Streptococcus sanguinis*. *Archives of Oral Biology* **57**: 940–947.
- Charalampakis, G. & Belibasakis, G.N. (2015) Microbiome of peri-implant infections: lessons from conventional, molecular and metagenomic analyses. *Virulence* **6**: 183–187.
- Charalampakis, G., Leonhardt, A., Rabe, P. & Dahlen, G. (2012) Clinical and microbiological characteristics of peri-implantitis cases: a retrospective multicentre study. *Clinical Oral Implants Research* **23**: 1045–1054.
- Costerton, J.W., Montanaro, L. & Arciola, C.R. (2005) Biofilm in implant infections: its production and regulation. *International Journal of Artificial Organs* **28**: 1062–1068.
- Faveri, M., Figueiredo, L.C., Shibli, J.A., Perez-Chaparro, P.J. & Feres, M. (2015) Microbiological diversity of peri-implantitis biofilms. *Advances in Experimental Medicine and Biology* **830**: 85–96.
- Gmur, R. & Guggenheim, B. (1983) Antigenic heterogeneity of bacteroides intermedius as recognized by monoclonal antibodies. *Infection and Immunity* **42**: 459–470.
- Guggenheim, B., Gmur, R., Galicia, J.C., Stathopoulou, P.G., Benakanakere, M.R., Meier, A., Thurnheer, T. & Kinane, D.F. (2009) In vitro modeling of host-parasite interactions: the 'subgingival' biofilm challenge of primary human epithelial cells. *BMC Microbiology* **9**: 280.
- Guggenheim, M., Shapiro, S., Gmur, R. & Guggenheim, B. (2001) Spatial arrangements and associative behavior of species in an in vitro oral biofilm model. *Applied and Environmental Microbiology* **67**: 1343–1350.
- Harris, L.G. & Richards, R.G. (2004) *Staphylococcus aureus* adhesion to different treated titanium surfaces. *Journal of Material Science and Material Medicine* **15**: 311–314.
- Heitz-Mayfield, L.J. & Lang, N.P. (2010) Comparative biology of chronic and aggressive periodontitis vs Peri-implantitis. *Periodontology 2000* **53**: 167–181.
- Leonhardt, A., Renvert, S. & Dahlen, G. (1999) Microbial findings at failing implants. *Clinical Oral Implants Research* **10**: 339–345.
- Mombelli, A. & Decaillet, F. (2011) The characteristics of biofilms in peri-implant disease. *Journal of Clinical Periodontology* **38**(Suppl 11): 203–213.
- Mombelli, A. & Lang, N.P. (1998) The diagnosis and treatment of peri-implantitis. *Periodontology 2000* **17**: 63–76.
- Otto, M., Echner, H., Voelter, W. & Gotz, F. (2001) Pheromone cross-inhibition between *Staphylococcus aureus* and *Staphylococcus epidermidis*. *Infection and Immunity* **69**: 1957–1960.
- Persson, G.R. & Renvert, S. (2014) Cluster of bacteria associated with peri-implantitis. *Clinical Implant Dentistry and Related Research* **16**: 783–793.
- Rams, T.E. & Link, C.C., Jr. (1983) Microbiology of failing dental implants in humans: electron microscopic observations. *Journal of Oral Implantology* **11**: 93–100.
- Rams, T.E., Roberts, T.W., Feik, D., Molzan, A.K. & Slots, J. (1991) Clinical and microbiological findings on newly inserted hydroxyapatite-coated and pure titanium human dental implants. *Clinical Oral Implants Research* **2**: 121–127.
- Renvert, S., Lindahl, C., Renvert, H. & Persson, G.R. (2008) Clinical and microbiological analysis of subjects treated with branemark or astratech implants: a 7-year follow-up study. *Clinical Oral Implants Research* **19**: 342–347.
- Renvert, S., Roos-Jansaker, A.M., Lindahl, C., Renvert, H. & Rutger Persson, G. (2007) Infection at titanium implants with or without a clinical diagnosis of inflammation. *Clinical Oral Implants Research* **18**: 509–516.
- Salvi, G.E., Furst, M.M., Lang, N.P. & Persson, G.R. (2008) One-year bacterial colonization patterns of *Staphylococcus aureus* and other bacteria at implants and adjacent teeth. *Clinical Oral Implants Research* **19**: 242–248.
- Thurnheer, T. & Belibasakis, G.N. (2015) Integration of non-oral bacteria into in vitro oral biofilms. *Virulence* **6**: 258–264.
- Thurnheer, T., Belibasakis, G.N. & Bostanci, N. (2014) Colonisation of gingival epithelia by subgingival biofilms in vitro: role of "red complex" bacteria. *Archives of Oral Biology* **59**: 977–986.
- Thurnheer, T., Gmur, R. & Guggenheim, B. (2004) Multiplex fish analysis of a six-species bacterial biofilm. *Journal of Microbiological Methods* **56**: 37–47.
- Willi, M., Belibasakis, G.N. & Bostanci, N. (2014) Expression and regulation of triggering receptor expressed on myeloid cells 1 in periodontal diseases. *Clinical and Experimental Immunology* **178**: 190–200.
- Zhuang, L.F., Watt, R.M., Mattheos, N., Si, M.S., Lai, H.C. & Lang, N.P. (2014) Periodontal and peri-implant microbiota in patients with healthy and inflamed periodontal and peri-implant tissues. *Clinical Oral Implants Research* doi:10.1111/clr.12508